INSTITUTE OF PHYSICS PUBLISHING JOURNAL OF PHYSICS B: ATOMIC, MOLECULAR AND OPTICAL PHYSICS

J. Phys. B: At. Mol. Opt. Phys. **39** (2006) L159–L166 doi:10.1088/0953-4075/39/7/L03

LETTER TO THE EDITOR

Alignment independence of the instantaneous ionization rate for nitrogen molecules

D Zeidler[1,2], A B Bardon[1,3], A Staudte[1,4], D M Villeneuve[1], R Dörner[4] and P B Corkum[1]

[1] National Research Council, 100 Sussex Drive, Ottawa, Ontario, K1A 0R6, Canada
[2] Carl Zeiss SMT AG, Carl-Zeiss-Str. 22, D-73447 Oberkochen, Germany
[3] Physics Department, Mount Allison University, Sackville, New Brunswick, E4 L 1E6, Canada
[4] Institut für Kernphysik, J W Goethe-Universität Frankfurt, Max-von-Laue-Str. 1, D-60438 Frankfurt, Germany

E-mail: Paul.Corkum@nrc.ca

Received 25 November 2005, in final form 27 November 2005
Published 20 March 2006
Online at stacks.iop.org/JPhysB/39/L159

Abstract

We investigate multiphoton single ionization with intense femtosecond laser fields in aligned nitrogen molecules. We find that the temporal structure of the electron wave packet released into the continuum by tunnelling ionization is independent of alignment and thus independent of the spatial structure of the orbital it originated from.

1. Introduction

The mechanism of electron recollision [1] has paved the way to experiments with attosecond temporal and Ångström spatial resolution. In a nutshell, the three-step model of electron recollision is described by (1) freeing an electron from an atom or molecule with a strong laser field that (2) drives the electron away from the core and back as soon as the oscillating laser field reverses its direction such that (3) the electron finally recollides with its parent ion. The key features of the returning electron pulse are (a) the coherence with respect to the parent orbital [2] and (b) its attosecond time duration [3]. The coherence has been used to observe the wavefunction of an orbital [2] for the first time and with Ångström precision, while the attosecond duration has led to the generation of attosecond optical pulses [4]. Moreover, the time dependence of the laser field that created the recollision electron impresses a phase dependent velocity boost to an electron that is released into this laser field [5]. This principle can be used to time resolve, with sub laser-cycle precision, double ionization stimulated by collisions [6] or photons [7].

In all these experiments, the crucial parameter that determines the experiment's temporal response function is the temporal structure of the returning wave packet. The final wave packet colliding with the parent ion is completely determined by the initial wave packet released into

the continuum via tunnelling ionization and its evolution in the Coulomb potential and the laser field. Of special interest is the time-dependent, space-averaged amplitude of the returning electron wave packet, as it provides a measure for the time-dependent current density seen by the parent ion. Its initial conditions are determined by the time-dependent ionization rate. For atoms, this rate depends on a number of variables, such as the field strength and the shape of the orbital the electron originated from.

Recently, molecules have become the focus of electron recollision experiments [2, 8]. Their simplest representatives, diatomic molecules, add another degree of freedom that influences the ionization rate, which is the angle between the electric field and the molecular axis [9, 10]. The immediate question "How does the returning wave packet depend on alignment?" is crucial for all recollision experiments on aligned targets. We need to know whether its temporal structure can be assumed to be independent of alignment.

We show that, to a good approximation, an unexpected simplicity exists in the temporal properties of the returning electron wavefunction: given that laser field and ionization potential are unchanged, the pure temporal structure of the returning wave packet does not depend on the spatial shape of the potential it originated from. In that case, the shape of the electron wave packet at its time of recollision only depends on the initial conditions at the time it appeared in the continuum. It is the laser field that entirely determines the temporal structure of the tunnel and thus the properties of the electron wave packet as it recollides.

We demonstrate in two steps that the temporal structure does not change: we show (a) that the kinetic energy of the direct, unscattered, low energy electrons is unambiguously mapped to the ionization time, yielding a relation between the kinetic energy spectrum and the time-dependent ionization rate. We then prove (b) that the shape of this spectrum produced in single ionization of aligned nitrogen molecules is insensitive to molecular alignment.

2. Electron energy spectrum and ionization time

We begin with (a). One possible and experimentally accessible piece of information is the above threshold ionization (ATI) energy spectrum, i.e., the ionization rate $w(E)$ as a function of the electron kinetic energy E. This ATI energy spectrum is already predicted well in the semi-classical model of ionization in low-frequency laser fields where the electron quantum mechanically tunnels through the potential barrier and is subsequently picked up by the laser field [1, 11]. The ionization rate is governed by the dipole matrix element for a transition of the ground state to a continuum state and the instantaneous laser field. The electron's motion in the laser field is then described by classical physics. How much information about the electron wave packet released into the continuum can be retrieved from the energy-resolved single electron ATI spectrum?

In linearly polarized light, the final momentum of the electron after the electron has become free is determined by the laser phase at which it appeared in the continuum. Solving the equation of motion of an electron in an oscillating laser field F with frequency ω and field envelope $F_0(t)$, i.e. $F(t) = F_0(t)\cos\omega t$, for the momentum of the electron in the direction of the laser field as $t \to \infty$ yields [1, 6, 12, 13]

$$p_\infty(t_{\mathrm{ion}}) = 2\sqrt{U_\mathrm{p}}\sin\omega t_{\mathrm{ion}} \tag{1}$$

with t_{ion} being the time at which the electron has been freed into the continuum and U_p the ponderomotive energy. We assume that the electrons are born with little excess momentum in all three spatial directions, such that the electron momentum is governed almost entirely by the laser field [14]. Experimentally, this can be achieved with a laser intensity well below the saturation intensity. In this case, the momentum perpendicular to the laser polarization

is small [15, 16], and the main contribution for the electron's kinetic energy originates from the momentum parallel to the laser field. We can restrict $\omega t_{\rm ion}$ to the first quarter laser cycle, i.e. $\omega t_{\rm ion} < \pi/2$, by symmetry considerations. We also neglect electron recollision by only looking at electrons with an energy below $U_{\rm p}$. Then equation (1) maps the final kinetic energy of the electron $E = p_\infty^2/2m$ and $t_{\rm ion}$. This streak camera principle has been key to many experiments on electron dynamics in atoms and molecules [6, 16–19]. It is also implicit in most attosecond experiments that induce ultrafast dynamics with an attosecond high harmonic generation (HHG) pulse and measure it by mapping the induced wave packet to a photoelectron wave packet that is characterized by streaking it with the IR laser field [4, 7].

This means that by measuring the kinetic energy of an electron which does not interact with the parent ion we indirectly measure its time of ionization. Therefore, measuring the ATI spectrum gives the spectrum of ionization times, or the space-averaged magnitude of the electron wave packet. Of course, we need to exclude the recollision electrons, as all electrons with more than $2\,U_{\rm p}$ kinetic energy and most electrons between $U_{\rm p}$ and $2\,U_{\rm p}$ must have recollided. Nevertheless, we still can infer on recollision because the motion of the electron is controlled by the same laser field in all cases. We can neglect Coulomb focusing since it mainly affects the electron wavepacket upon return to the parent ion whereas the initial tunnelling creates the wavepacket rather far away from the ion [20].

3. Electron energy spectrum and molecular alignment: theory

We now theoretically demonstrate (b) by showing that the shape of the electron kinetic energy spectrum does not depend on the angle θ between the molecular axis and the laser polarization. We do this within the framework of tunnelling ionization theory by Ammosov, Delone and Krainov, adapted to molecules (molecular ADK theory) [10]. This model has been experimentally confirmed by Litvinyuk *et al* [9]. However, the temporal dependence of this theory has not been confirmed experimentally up to now.

We start by noting that the angle and field dependent ionization rate $w(F,\theta)$ is given by [10]

$$w(F,\theta) = \sum_m B^2(m,\theta) w_m(F) \tag{2}$$

with the static ionization rate

$$w_m(F) = \frac{(2I_{\rm p})^{-\frac{1}{2}\left(\frac{2Z}{\sqrt{2I_{\rm p}}}-1\right)}}{2^{|m|}|m|!}\left(\frac{2(2I_p)^{3/2}}{F}\right)^{\frac{2Z}{\sqrt{2I_{\rm p}}}-1-|m|}\exp\left[-\frac{2(2I_{\rm p})^{3/2}}{3F}\right] \tag{3}$$

and

$$B(m,\theta) = \sum_l C_l D^l_{m,m'}(0,\theta,0)(-1)^m\sqrt{\frac{(2l+1)(l+|m|)!}{2(l-|m|)!}}. \tag{4}$$

Here, $I_{\rm p}$ is the ionization potential, Z the ion charge, and m the magnetic quantum number of the orbital the electron is ejected from. The C_l are coefficients that depend on the molecular orbital the electron originates from, and $D^l_{m,m'}$ is the rotation matrix [10]. Equations (3) and (4) already show that the largest part of the field dependence of the ionization rate is contained in the exponential factor which is independent of θ. A possible mixed dependence on field and orientation can thus only arise in the summation in equation (2).

To check this, figure 1 shows the ionization rate as a function of electron energy for $\theta = 0^\circ$ and $\theta = 90^\circ$ for nitrogen calculated from equation (2) at an electric field F_0 corresponding to an intensity of 1.2×10^{14} W cm^{-2}. By varying the electric field, we effectively control $t_{\rm ion}$.

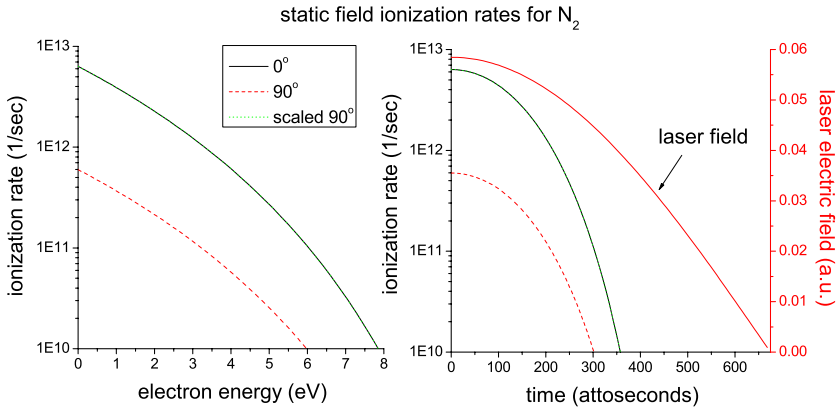

Figure 1. Ionization rates $w(F(t_{\rm ion}), \theta)$ for $\theta = 0^\circ$ (molecular axis parallel to ionizing laser field) and $\theta = 90^\circ$ (molecular axis perpendicular to ionizing laser field) as given by equation (2). Left panel: on the abscissa the instantaneous laser field strength $F(t_{\rm ion})$ has been mapped onto the final electron energy using equation (1). Right panel: ionization rate as a function of $t_{\rm ion}$ relative to the field maximum corresponding to a peak intensity of 1.210^{14} W cm^{-2}. The ratio of the two ionization rates is independent of tunnelling time.

(This figure is in colour only in the electronic version)

We then use equation (1) to map the ionization time to the final electron kinetic energy. The ratio between the two curves is constant with an accuracy better than $1/1000$, which means that the shape of the direct electron spectrum is unaffected by molecular alignment. This, in return, means that the wave packets released into the continuum are independent of molecular alignment.

4. Electron energy spectrum and molecular alignment: experiment

We now show that the shape of $w(E)$ is independent of alignment in the experiment as well. The experimental set-up has been described in [21]. Here, we give some more details on the experiment.

Ultrashort pulses from a Ti:Sa regenerative amplifier (∼40 fs, 800 nm, 30 kHz, 5 μJ) were fed through a Mach-Zehnder interferometer to produce two pulses with adjustable delay. We use polarizers to split and recombine the beams, avoiding the 50% loss that an interferometer with dielectric beam splitters would produce. A half-wave plate in front of the interferometer determines the splitting ratio in its two arms. The time difference between the two pulses was set with a motorized delay line.

Both pulses were focused into a supersonic gas jet with an $f = 50$ mm, $f/2$ parabolic mirror. For the gas jet, N_2 at a backing pressure of 2 bar was introduced through a 30 μm nozzle into a differentially pumped source chamber. The jet passed through a 1 mm skimmer into the detection chamber. The background pressure of the detection chamber was 2×10^{-10} mbar if the jet was off; it increased by about one order of magnitude when the molecular jet was sent into the detection chamber.

The vertically polarized alignment (or pump) pulse was stretched to about 60 fs with a 15 mm quartz block: optimal alignment is achieved for comparable pulse duration and alignment time of the molecules. Furthermore, we placed an aperture inside the alignment beam to ensure that its focal volume was larger than that of the ionization beam. Finally, we worked at the highest possible intensity with a low ionization background produced by the

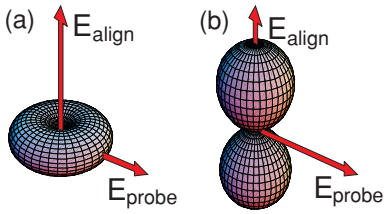

Figure 2.

alignment pulses alone ($< 1\%$) compared to the ionization pulses. Knowing the intensity of the ionization pulse, we could deduce the pump intensity to be $(2.5 \pm 1) \times 10^{13}$ W cm^{-2} from the intensity dependence of argon ionization yields as well as theoretical molecular ionization rates for N_2. This value agrees well with an intensity estimate from pulse length, pulse energy and focus area.

The horizontally polarized ionization pulse was neither clipped nor chirped. From the momentum distribution of the electrons during single ionization, we calculate its intensity to be $(1.2 \pm 0.2) \times 10^{14}$ W cm^{-2} [15].

We used cold target recoil ion momentum spectroscopy (COLTRIMS) to determine the momenta of electrons and ions [22, 23]. They were directed via a uniform electric field of 5.6 V cm^{-1} and a magnetic field of 11.0 G towards two microchannel plates with delay-line readout. From time-of-flight and position on the detectors, the three-dimensional momentum vector for each particle was obtained. For the electrons, the extraction length was 6.3 cm and the field-free length was 14.6 cm, whereas the corresponding lengths for the ions were 22.3 cm and 43.5 cm, respectively. The single ionization channel can also be used to measure the momentum resolution of the system via momentum conservation. It is ± 0.18 au along the spectrometer axis, which is parallel to the direction of the ionization laser, ± 0.37 au along the propagation direction of the laser, and ± 1.37 au along the jet direction, i.e., parallel to the direction of the alignment laser. From the last value, we deduce a translational jet temperature of 6 K. The rotational temperature can be estimated to be only slightly above this temperature [24]. The settings of electric and magnetic fields yielded 4π solid angle for electrons up to 42 eV.

The electron count rate was 0.3 per shot and the ion rate 0.1. For single ionization, real coincidences are identified by momentum conservation between ion and electron. A valid event required one N_2^+ ion and one electron as well as their momentum conservation.

The pump pulse creates a rotational wave packet in the nitrogen ensemble [25]. The wave packet quickly dephases, and rephases at half multiples of $\tau = 1/(2B_e) \approx 8$ ps. We use a delay of $\approx$4 ps where the angular distribution of the wave packet first peaks parallel to the alignment pulse polarization and then in a disk shape perpendicular to the alignment pulse shortly afterwards [26]. Throughout this paper, though, we define parallel (figure 2(a)) and perpendicular (figure 2(b)) with respect to the ionization pulse polarization. The angle-dependent ionization rate thus minimizes at 3.93 ps when the ensemble is aligned perpendicular to the ionization pulse and maximizes at 4.30 ps when it is parallel [9, 10]. Compared to unaligned molecules, we observe an increase and decrease, respectively, by more than 8% in the direct total count rate when switching the delay between 4.30 ps and 3.93 ps.

We verified that the first pulse produces aligned molecules with two independent methods: the first, indirect method relies on the alignment-dependent ionization rate of molecules [10]. We introduced a neon/nitrogen gas mixture in the jet and used the neon ionization yield as a reference to find relative yields for the different time delays, i.e. alignments of the molecules.

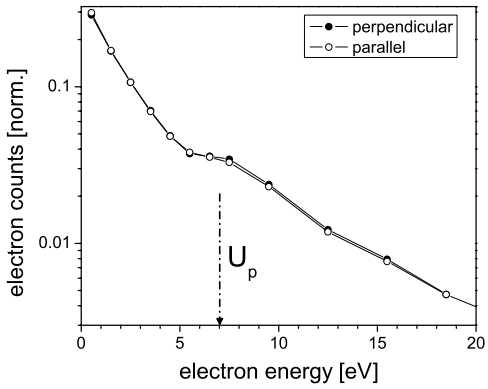

Figure 3. Electron counts for perpendicular and parallel molecules, normalized by the total number of counts, as a function of electron energy. Each valid event required exactly one electron and one ion to be observed. Though electron energies as high as 70 eV have been observed, we only show electrons up to 20 eV since energy range of interest in this letter is between 0 and $2U_p$. We can detect electrons up to 42 eV with 4π solid angle. The line in the figure indicates the ponderomotive energy $U_p \approx 7$ eV. The error bars in x direction are smaller than the bin size, and the error bars in the y direction are smaller than the size of the dots. See the text for details on the normalization of the curves.

We observed 19% more N_2^{1+} ions and 30% more N_2^{2+} ions when the molecules are aligned parallel. This is in good agreement with previously published results [9].

Second, we detected all N^+ ions from the $N_2 \rightarrow N^+ + N$ channel if they were emitted within a small angle within the spectrometer axis, i.e., parallel to the ionizing field. This method provides a direct measure of alignment, as the fragments are emitted in the direction of the molecular axis. For the two time delays, we normalize the number of N^+ fragments within 6° of the laser polarization to the total number of observed N^+ fragments. Per observed N^+ fragment, we find 24% more N^+ events within the direction of the ionizing laser for parallel molecules.

For single ionization of nitrogen molecules, $N_2 \rightarrow N_2^+ + e$, figure 3 shows electron distributions for perpendicular and parallel aligned molecules plotted as a function of the electron energy, computed from the full 3D momentum vector of the electrons. This is feasible because the lateral electron momentum is low. Each data point in each curve has been normalized to the total number of single ionization events in the experiment corresponding to this curve, such that both data sets are normalized to the same number numbers of events. In doing so, we suppress the effect of different total ionization yield for different alignments. We could have also normalized the curves by the number of laser shots in the corresponding experiment, which would lead to a mere shift between them, making a comparison more difficult.

Measured over more than two orders of magnitude, the agreement of the two curves plotted for the same number of ionization events is remarkable, especially since the total rate varies by 19%. Since we are dealing with alignment distributions in the experiment, the contrast in the ionization yields is lower than molecular ADK predicts. As a bottom line, the shape of low energy part of the electron spectrum does not depend on the alignment of the N_2 molecules. Compared to the theoretical curves, the presence of the 'knee' at around 7 eV is explained by the onset of electron recollision that opens further ionization pathways [27]. Electron recollision has not yet been included in the present molecular ADK model, which explains the qualitative differences between theoretical and experimental curves.

5. Conclusions

In conclusion, the independence of the spectrum on alignment of the N_2 molecules shows that, although electron wave packets released into the continuum at different alignments differ in their magnitude, their temporal shape is the same. Given that the parameters laser intensity and ionization potential are unchanged, the shape of the orbital the electron originated from contributes only little: temporally, the two tunnels are alike. This simplicity—astonishing, as the shape and size of the highest occupied molecular orbital differs for perpendicular and parallel N_2 molecules—will be of great importance for the interpretation of experiments where the time-dependence of the returning wave packet determines the response function of the experiment. Further experiments on the single ionization of aligned oxygen molecules suggest that this might be valid for molecules with different symmetry of the highest occupied molecular orbital (HOMO) as well, which will be the subject of a further paper.

Acknowledgments

We thank T Brabec, M Meckel, O Geß ner and M Ivanov for valuable discussions. A B thanks the NRC WES program, A S the Studienstiftung des deutschen Volkes, and D Z the Alexander von Humboldt-Stiftung for financial support.

References

[1] Corkum P B 1993 Plasma perspective on strong-field multiphoton ionization *Phys. Rev. Lett.* **71** 1994
[2] Itatani J, Levesque J, Zeidler D, Niikura H, Pépin H, Kieffer J-C, Corkum P B and Villeneuve D M 2004 Tomographic imaging of molecular orbitals *Nature* **432** 867
[3] Niikura Hiromichi, Legare F, Hasbani R, Bandrauk A D, Ivanov Misha Yu, Villeneuve D M and Corkum P B 2002 Sub-laser-cycle electron pulses for probing molecular dynamics *Nature* **417** 917
[4] Kienberger R *et al* 2004 Atomic transient recorder *Nature* **427** 817
[5] Itatani J, Quéré F, Yudin G L, Ivanov M Yu, Krausz F and Corkum P B 2002 Attosecond streak camera *Phys. Rev. Lett.* **88** 173903
[6] Weckenbrock M *et al* 2004 *Phys. Rev. Lett.* **92** 213002
[7] Drescher M, Hentschel M, Kienberger R, Uiberacker M, Yakovlev V, Scrinzi A, Westerwalbesloh Th, Kleineberg U, Heinzmann U and Krausz F 2002 Time-resolved atomic inner-shell spectroscopy *Nature* **419** 807
[8] Eremina E, Liu X, Rottke H, Sandner W, Schätzel M G, Dreischuh A, Paulus G G, Walther H, Moshammer R and Ullrich J 2004 Influence of molecular structure on double ionization of N_2 and O_2 by high intensity ultrashort laser pulses *Phys. Rev. Lett.* **92** 173001
[9] Litvinyuk I V, Lee Kevin F, Dooley P W, Rayner D M, Villeneuve D M and Corkum P B 2003 Alignment-dependant strong field ionization of molecules *Phys. Rev. Lett.* **90** 23303
[10] Tong X M, Zhao Z X and Lin C D 2002 Theory of molecular tunneling ionization *Phys. Rev.* A **66** 033402
[11] Lewenstein M, Balcou Ph, Ivanov M Yu, L'Huiller Anne and Corkum P B 1994 Theory of high-harmonic generation by low-frequency laser fields *Phys. Rev.* A **49** 2117
[12] Corkum P B, Burnett N H and Brunel F 1989 Above-threshold ionization in the long-wavelength limit *Phys. Rev. Lett.* **62** 1259
[13] Weber Th, Glessen H, Weckenbrock M, Urbasch G, Staudte A, Spielberger L, Jagutzki O, Mergel V, Vollmer M and Dörner R 2000 Correlated electron emission in multiphoton double ionization *Nature* **405** 658–61
[14] Delone N B and Krainov V P 1994 *Multiphoton Processes in Atoms* (Berlin: Springer)
[15] Zeidler D *et al* 2004 *Proc. SPIE* **5579** 708
[16] Weckenbrock M, Becker A, Staudte A, Kammer S, Smolarski M, Bhardwaj V R, Rayner D M, Villeneuve D M, Corkum P B and Doerner R 2003 Electron-electron momentum exchange in strong-field double ionization *Phys. Rev. Lett* **91** 123004
[17] Eremina E *et al* 2003 Laser-induced non-sequential double ionization investigated at and below the threshold for electron impact ionization *J. Phys. B: At. Mol. Opt. Phys.* **36** 3269

[18] Feuerstein B *et al* 2001 Separation of the recollision mechanisms in nonsequential strong field double ionization of Ar: the role of excitation tunneling *Phys. Rev. Lett.* **87** 043003
[19] Moshammer R *et al* 2000 Momentum distributions of ne(n+) ions created by an intense ultrashort laser pulse *Phys. Rev. Lett.* **84** 447
[20] Comtois D, Zeidler D, Pepin H, Kieffer J C, Villeneuve D M and Corkum P B 2005 Observation of coulomb focusing in tunneling ionization of noble gases *J. Phys. B: At. Mol. Opt. Phys.* **38** 1923
[21] Zeidler D, Staudte A, Bardon A, Dörner R, Villeneuve D M and Corkum P B 2005 *Phys. Rev. Lett.* **95** 203003
[22] Dörner R, Mergel V, Jagutzki O, Spielberger L, Ullrich J, Moshammer R and Schmidt-Böcking H 2000 *Phys. Rep.* **330** 192
[23] Ullrich J, Moshammer R, Dorn A, Dörner R, Schmidt L Ph and Schmidt-Böcking H 2003 *Rep. Prog. Phys.* **66** 1463
[24] Ramos A, Tejeda G, Fernandez J M and Montero S 2002 Rotational-translational state-to-state collisional rate constants of N_2 at low temperature ($3 < T < 16$ K) *Phys. Rev.* A **66** 022702
[25] Dooley P W, Litvinyuk I V, Lee Kevin F, Rayner D M, Spanner M, Villeneuve D M and Corkum P B 2003 Direct imaging of rotational wave packet dynamics of diatomic molecules *Phys. Rev.* A **68** 023406
[26] Rosca-Pruna F and Vrakking M J J 2001 Experimental observation of revival structures in picosecond laser-induced alignment of I_2 *Phys. Rev. Lett.* **87** 153902
[27] Walker B, Sheehy B, Kulander K C and DiMauro L F 1996 Elastic rescattering in the strong field tunneling limit *Phys. Rev. Lett.* **77** 5031